Fibers and Polymers
https://doi.org/10.1007/s12221-024-00516-5

Online ISSN 1875-0052
Print ISSN 1229-9197

REGULAR ARTICLE

A New Lotus-Leaf-Inspired Beaded Nanofiber Strategy for the Development of Cryogel/Nanofiber Hybrid Structures

Dilayda Kanmaz[1,2] · **Bilgen Osman**[2,3] · **Esra Karaca**[1,2]

Received: 11 December 2023 / Revised: 18 February 2024 / Accepted: 22 February 2024
© The Author(s) 2024

Abstract

In this study, a cryogel/nanofiber hybrid material was developed using a new lotus-leaf-inspired strategy. The lotus effect was generated via beaded poly(ε-caprolactone) (PCL) nanofibers produced from the 9 wt% PCL solution with low viscosity and high surface tension via electrospinning. A poly(hydroxyethyl methacrylate) (PHEMA) cryogel layer was constructed through polymerization onto the beaded PCL nanofibrous mat. The thickness of the PHEMA cryogel/beaded PCL nanofiber hybrid material was 3.19 ± 0.07 mm. Morphological characterization studies of the hybrid material were conducted by scanning electron microscopy (SEM). The mean diameter of the beaded PCL nanofibers was 97.22 ± 21.18 nm. The lotus effect created by the beaded PCL nanofibers was investigated by water contact angle (WCA) measurements. The WCA of beadless and beaded PCL nanofibers was 93.42° ± 1.4° and 117.97° ± 5.04°, respectively. The PHEMA cryogel layer was chemically characterized via Fourier transform infrared spectroscopy (FTIR) analysis and the specific groups belonging to 2-hydroxyethyl methacrylate (HEMA) was observed. The porosity of the PHEMA cryogel layer was determined via mercury porosimetry. The total porosity of the PHEMA cryogel was 64.42%, and the pore sizes were in the range of 5–200 µm. Swelling kinetics of the PHEMA cryogel/beaded PCL nanofiber hybrid material were also investigated and compared to those of PHEMA cryogel and beaded PCL nanofibers. The maximum swelling ratio of the hybrid material was 509.69% and reached after 180 min. The developed PHEMA cryogel/beaded PCL nanofiber hybrid material met the criteria required for layered structures and biomedical applications whereby its eligible stability, morphology, porosity, and swelling capacity. Consequently, the lotus-leaf-inspired strategy was successful in constructing the cryogel/nanofiber hybrid materials.

Keywords Hybrid material · Beaded nanofiber · Cryogel · PHEMA · PCL

1 Introduction

Porous polymeric materials are especially preferred in biomedical applications due to their producibility in different forms such as nanofiber, hydrogel, film, and sponge [1–4]. Among them, nanofibers, fibers with diameters ranging from 50 to 1000 nm (preferably 50–500 nm), have been widely used in many areas such as defense, aerospace, filtration, electronic, agriculture, composite, food, and textile besides biomedical and tissue engineering applications [5–12]. Electrospinning is a simple, efficient, and economical method to produce nanofibers from polymer solutions or melts [13, 14]. The characteristic features of the nanofibers are adjustable porosity, ultra-high specific surface area, good mechanical properties (depending on the polymer), changeable surface characteristics, and mimicable extracellular matrix [15–18].

Hybrid materials are up-and-coming to obtain multifunctionality in biomaterials, enabling them to benefit

✉ Esra Karaca
ekaraca@uludag.edu.tr

Dilayda Kanmaz
dilaydakanmaz@uludag.edu.tr

Bilgen Osman
bilgeno@uludag.edu.tr

[1] Department of Textile Engineering, Faculty of Engineering, Bursa Uludag University, Gorukle, 16059 Bursa, Turkey

[2] Department of Biomaterials, Graduate School of Natural and Applied Sciences, Bursa Uludag University, Gorukle, 16059 Bursa, Turkey

[3] Department of Chemistry, Faculty of Arts and Science, Bursa Uludag University, Gorukle, 16059 Bursa, Turkey

Published online: 05 March 2024

from different structural and chemical components [19]. Recently, many studies have been conducted to construct hybrid structures by combining hydrogels, sponges, films, and nanofibers. Various methods have been reported for preparing hybrid materials, including electrospun layers. A three-layered nanofibrous scaffold was produced by Huang et al. [20] via electrospinning for skin reconstruction using poly(ε-caprolactone) (PCL), cellulose acetate, and chitosan. Pal et al. [21] created a bilayer nanofibrous structure as a skin graft for burn wounds. An electrospinning process was applied for the PCL and chitosan mixture, followed by collagen coating by freeze-drying method to obtain a cotton-wool-like fluffy 3D structure. PCL-chitosan emulsion was deposited on the nanofibrous scaffold as a second layer. Bilayer scaffolds from poly (l-lactic acid) (PLLA) were produced by a new electrospinning process for tissue regeneration with a distinctive collector design [22]. Lin et al. [23] constructed a tri-layer skin composite from chitosan/polyvinyl alcohol (PVA)/pectin by electrospinning and freeze-drying methods.

Recently, nanofiber–hydrogel hybrid materials have attracted significant attention. Wu et al. [24] produced multilayer PCL nanofiber–alginate hydrogel structures for drug release. An alginate hydrogel was produced onto the PCL electrospun nanofibrous mat wetted with $CaCl_2$ solution. A tri-layered scaffold was prepared by casting, electrospinning, and lyophilization as skin tissue for deep wound healing [25]. The top layer, middle layer, and bottom layer of the scaffold were produced from PCL film, PCL nanofibrous mat, and gelatin hydrogel using casting, electrospinning, and lyophilization methods, respectively. Franco et al. [26] built a bilayer scaffold consisting of PCL/poly (lactic-co-glycolic acid) (PLGA) nanofibrous mat and chitosan/gelatin hydrogel using two methods. The first method was to perform electrospinning on the hydrogel. In the second method, the hydrogel was produced on nanofibrous mat.

The hybrid materials constructed from hydrogel layers have also been reported recently. Zonari et al. [27] produced bilayer constructs from polihidroksibutirat-kohidroksivalerat (PHBV) by solution casting and freeze-drying methods for skin wound healing. Nicholas et al. [28] created bilayer hydrogel from pullulan-gelatin by freeze-drying method for skin regeneration. A bilayer dermal scaffold from collagen, chitosan, and silicone was produced by the freeze-drying process for wounds and burns [29]. A tri-layer wound dressing comprising polypropylene (PP)-poly-*N*-isopropyacrylamide (PNIPAAm)-gelatin/hyaluronan/chondroitin-6-sulfate was reported as the artificial skin for extensive burn injury. The PP-PNIPAAm double-layer structure was prepared by immersing non-woven fabric of PP activated with a CVD plasma chamber. γ-Irradiation was used to graft PNIPAAm onto the surface. The bilayer structure was soaked into a gelatin solution followed by UV light exposure. The third layer was prepared by soaking the structure in hyaluronan and chondroitin-6-sulfate solution to form the tri-layer structure [30]. A bilayer skin scaffold from sodium alginate, collagen, and fibrinogen was also produced by a freeze-drying method [31].

Cryogels are gel matrices of interconnected pores ranging from 10 to 200 μm, prepared with partially frozen monomer or polymer solutions. Super-macroporous structure, high water absorption, rapid swelling mechanism, mechanical stability and viscoelasticity, chemical stability and modifiability, high compressibility, easy production, and long shelf life are among the characteristic features of cryogels [32–34]. Since cryogels are versatile materials, they have been preferred to use in applications such as tissue engineering [35], protein purification [36], chromatography [37], controlled drug release [38], wound repair [39], and water purification [40]. Nanofibers and cryogels from various polymers can be combined to construct a hybrid membrane promising hierarchical micro/nanopores and good mechanical properties. Although the advantages of nanofibers and cryogels have been profited separately in the biomedical field, a limited number of biomaterials [41] that benefit from the advantages of both materials simultaneously have been reported because of the difficulty in combining different structures. Cross-linking was required to interact the cryogel and nanofibrous structures [42] permanently. However, studies on nanofibers dispersed in aerogel structures [43–45] and hydrogel-nanofiber layered structures [46–48] have attracted attention in recent years. It is challenging to combine the three-dimensional cryogel surface with the almost two-dimensional nanofibrous mat to form a hybrid material due to the brittleness of the cryogel structure in the dry state and the interpenetration of the polymeric materials without creating an intersection or adhesion. The only study on nanofiber–hydrogel hybrid material preparation was reported by Sa'adon et al. [49], who produced dual-layer PVA nanofiber/cryogel by electrospinning and freezing–thawing method as a transdermal patch. PVA solution was poured onto the PVA nanofibrous mat, and the bilayer structure was frozen and melted three to five times. However, as far as we know, there is no report on preparing cryogel–nanofiber hybrid material in which cryogels are prepared from partially frozen monomer solutions.

Nature is an excellent, inspiring source for designing and producing hybrid materials. The lotus leaf is the most well-known sample of superhydrophobic surfaces due to the micrometer-sized papillae on its surface. Various methods can be used to prepare rough surfaces that will create a lotus effect. One of them is constructing beaded (bead-on-string) nanofibers by electrospinning [50, 51]. The beaded nanofibers commonly observed during electrospinning are usually considered by-products of the process [52, 53]. At first, the beads on the electrospun fibers were thought of

as undesired structural defects that could affect the performance of nanofibers [54]. However, this phenomenon has changed considerably in recent years [55]. Beaded nanofibers are advantageous in applications such as air filtration [56], tissue engineering [57], drug delivery [58], oil/water separation [59], electronic device [60], moisture sensor [61], and superhydrophobic materials [62].

In this study, a new lotus-leaf-inspired beaded nanofiber strategy was developed to prepare a cryogel/nanofiber hybrid structure. The cryogel/nanofiber hybrid material was prepared by constructing a poly(2-hydroxyethyl methacrylate) (PHEMA) cryogel structure on the surface of the electrospun beaded PCL nanofibers. PHEMA is a hydrophilic polymer that is physiologically compatible, mechanically strong, chemically and biologically stable [63], and biocompatible with blood. PCL, one of the aliphatic polymers, is nontoxic, biocompatible, easily processable, soluble in various solvents, and has desirable mechanical properties. Since approved by the Food and Drug Administration (FDA), PCL is frequently used in biomedical applications such as scaffolds, sutures, prosthetics, and drug delivery systems. PCL is also a suitable candidate for hydrophobic nanofibrous surface fabrication [64, 65]. The morphological of the beaded structure of PCL nanofibers enabling to construct the PHEMA cryogel/PCL nanofiber hybrid material was investigated by scanning electron microscopy (SEM). The PHEMA cryogel layer was chemically characterized via Fourier transform infrared spectroscopy (FTIR) analysis to demonstrate that 2-hydroxyethyl methacrylate (HEMA) monomer was successfully crosslinked by *N*,*N*′-methylenebis(acrylamide) (MBAAm). Water contact angle (WCA) measurements were used to evaluate the hydrophilicity of PCL nanofibers (beaded and beadless). The swelling ratios of PCL nanofibers, PHEMA cryogel, and PHEMA cryogel/beaded PCL nanofiber hybrid material were detailedly investigated to determine the application potential of the hybrid structure as a biomaterial.

2 Materials and Methods

2.1 Materials

PCL (molecular weight of 80.000 g/mol), dimethylformamide (DMF), and ammonium persulfate (APS) were purchased from Sigma-Aldrich (St. Louis, USA). Tetrahydrofuran (THF) was obtained from Tekkim (Bursa, Turkey). HEMA was obtained from Fluka A.G. (Buchs, Switzerland). *N*, *N*, *N*′, *N*′-tetramethylethylenediamine (TEMED) and MBAAm were supplied from Merck (Darmstadt, Germany). All chemicals were used without further purification. Elga Flex3 water purification system (Veolia Water Solutions & Technologies, France) was used to prepare purified water.

2.2 Preparation of the Electrospun PCL Nanofibers

Two different PCL nanofibers (beaded and beadless) were prepared via electrospinning. For this purpose, PCL solutions at concentrations of 9% (*w*/*v*) for producing beaded PCL nanofibers and 12% (*w*/*v*) for producing beadless PCL nanofibers were prepared in a DMF:THF solvent system (1:1, *v*:*v*). The binary solvent system was used to prepare a homogeneous and less toxic solution, to enhance the electrospinnability, and adjust the structure and morphology of the nanofibers and the beads [66, 67]. The solutions were magnetically stirred at 50 °C for 24 h. The viscosity and surface tension of the polymer solutions were determined before the electrospinning process. RV-DV II + Pro Extra Brookfield viscometer was used to determine viscosity at a 100 rpm stirring rate. KSV-The Modular CAM 200 tensiometer was used to determine the surface tension.

The PCL nanofibrous mats were produced using an electrospinning system (Inovenso Technology Inc., Turkey). A syringe with a 21-gauge needle was used as the feeding unit. A cylinder rotating at 100 rpm was used as the collector. The electrospinning was performed at room temperature. The nanofibrous mat was produced from the electrospinning solution of 10 ml. Process parameters of the electrospinning are given in Table 1.

2.3 Preparation of the Cryogel/Nanofiber Hybrid Material

The hybrid material was constructed from PHEMA cryogel and beaded PCL nanofibrous mat. For this purpose, two glass plates were first positioned with a gap of 3.77 mm, and the beaded PCL nanofibrous mat was placed between the glass plates. To prepare the cryogelation mixture, MBAAm was added to the deionized water, and then, the solution was added to the 1.3 mL of HEMA monomer. After adding

Table 1 Electrospinning process parameters

PCL concentration (%)	Feed rate (mL/h)	Applied voltage (kV)	Needle-tip-to-collector distance (cm)
9 (for beaded PCL nanofibers)	1	15	15
12 (for beadless PCL nanofibers)	1	24	15

0.02 g APS to the mixture in an ice bath, TEMED was put into the solution, and the cryogelation mixture was poured between the glass plates, including a beaded PCL nanofibrous mat. Polymerization was carried out at − 18 °C for 24 h. The prepared cryogel/nanofiber hybrid material was thawed at room temperature and then washed with deionized water to remove unreacted monomers. PHEMA cryogel/PCL nanofiber (beadless) hybrid material was also constructed via the same procedure using a beadless PCL nanofibrous mat.

2.4 Characterization Studies

2.4.1 SEM and FTIR Analyses

The morphologies of the PHEMA cryogel, PCL nanofibers (beaded and beadless), and cryogel/nanofiber hybrid materials were observed using Carl Zeiss AG-EVO 40 XVP Scanning Electron Microscope at 20 kV. The samples were coated with gold–palladium before SEM analysis. The PCL nanofibers' mean nanofiber diameter and diameter distribution were determined from 100 random measurements using ImageJ software on SEM images. Optical images of the PHEMA cryogel/PCL nanofibers (beaded and beadless) hybrid materials were taken by MSHOT MS60 digital microscope. FTIR analysis of PHEMA cryogel was conducted by an FTIR spectrometer (Shimadzu IR Tracer-100) within the frequency range of 400–4000 $cm.^{-1}$

2.4.2 Thickness Measurements

The thickness of PHEMA cryogel/beaded PCL nanofiber hybrid material was measured using INSIZE Digital Micrometer at five different locations.

2.4.3 WCA Measurements

The hydrophilicity of the PCL nanofibrous mats (beaded and beadless) was investigated via KSV-The Modular CAM 200 Contact Angle Measurement System measuring the WCA. The measurements were replicated three times.

2.4.4 Mercury Porosimetry Analysis

The porosity and pore size distribution of PHEMA cryogel was determined through mercury porosimetry analysis using Quantachrome Corporation, Poremaster 60. The applied pressure was 25 psi.

2.4.5 Swelling Studies

The swelling behaviors of the PHEMA cryogel, beaded PCL nanofibers, and PHEMA cryogel/beaded PCL nanofiber hybrid material were assessed in pure water at 25 °C at specific time intervals. The dried samples (2 cm × 2 cm) were weighted (Wd) and then immersed in pure water. The excess water of the samples was removed with a filter paper and weighed (Ws). The experiment was done in triplicates for each material. The swelling ratios (%) were calculated using Eq. (1):

$$\text{Swelling Ratio}(\%) = \left(\frac{Ws - \text{Wd}}{Wd}\right) \times 100. \quad (1)$$

3 Results and Discussion

3.1 Properties of the Cryogel/Nanofiber Hybrid Material

3.1.1 Morphological Characteristics

This study's main approach was to create a lotus-leaf effect to ensure the successful attachment of the cryogel layer (PHEMA) to the nanofiber layer (PCL), benefiting the beaded structure. The procedure applied to construct the PHEMA cryogel/beaded PCL nanofiber hybrid material is given in Fig. 1. It has been known that the lotus-leaf effect is surface roughness-induced hydrophobicity. Wenzel [68], and Cassie and Baxter [69] reported that a surface's rough and porous structure combined with a low surface energy can contribute to its hydrophobicity. The surface of the lotus leaf is chemically constructed of wax. Structurally, it has two levels of roughness consisting of nano-scale bumps on the surface of microscale protrusions that enable the trapping of air underneath water droplets, thereby contributing to a well-designed superhydrophobic surface [70]. In this study, PCL, which has low surface energy, was used to produce beaded nanofibers creating surface roughness-induced hydrophobicity due to the air trapping under water droplets. In other words, the wettability of the nanofibers' surface with cryogel solution decreased due to the micro-sized beads on the PCL nanofibers. At the same time, the contact area increased due to the roughness created by micro-sized beads. SEM analyses were conducted for PCL nanofibers (beadless and beaded), PHEMA cryogel, and cryogel/nanofiber hybrid material to demonstrate the applied procedure's applicability. The SEM images of the beadless and beaded PCL nanofibers are given in Fig. 2a and b, respectively.

The main factors in forming beaded nanofibers are the electrospinning solution's viscosity and surface tension and the electrospinning jet's net charge density. Low viscosity, net charge density, and high surface tension favor the formation of fibers with beads [52, 71]. At a low concentration, the viscosity of the solution is low, while the surface tension is relatively high. For a jet to be formed from the solution, the

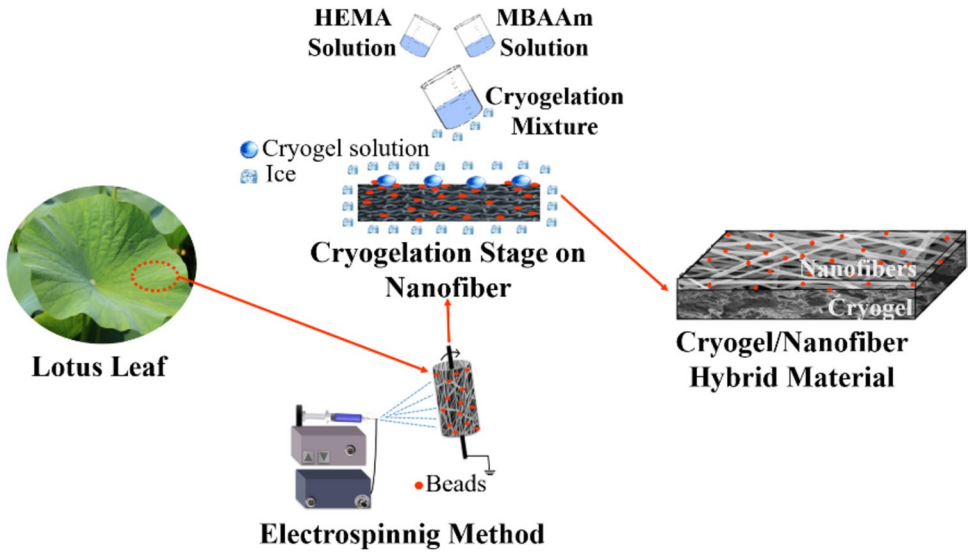

Fig. 1 The procedure applied in the study

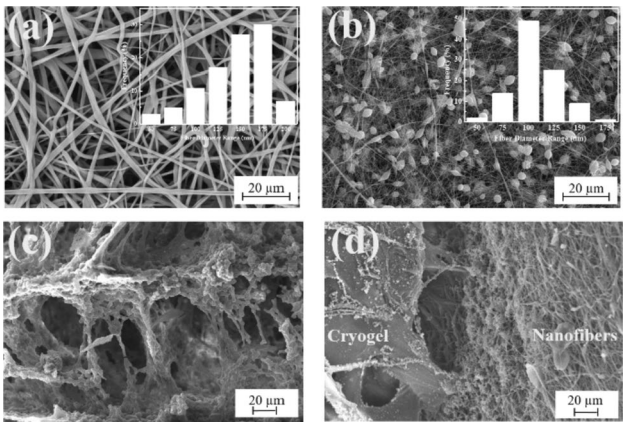

Fig. 2 SEM images; **a** the beadless PCL nanofibers (2000×), **b** the beaded PCL nanofibers (2000×), **c** the PHEMA cryogel (1000×), **d** the cross-section of PHEMA cryogel/beaded PCL nanofiber hybrid material (1000×)

net charge density carried by the jet must be increased, the electrostatic forces must overcome the surface tension of the solution, and thus, the droplet must be stretched. During the electrospinning, the solution with low viscosity may break up into droplets due to high surface tension, and small spherical beads among the fibers (beads-on-string morphology) are formed [54, 72]. The viscosity and surface tension of the 12 wt% PCL solution prepared to produce smooth, continuous, and beadless nanofibers (Fig. 2a) were measured as 352 cp and 30.24 mN/m, respectively. The 9 wt% PCL solution had a low viscosity of 249.6 cp and a high surface tension of 43.87 mN/m to support the beaded nanofiber formation (Fig. 2b). It has been reported that fiber formation occurred from PCL electrospinning solution of 10–15% concentration and the nanofibers did not contain beads. The beads have been observed widely in PCL nanofibers produced from solutions with 10 wt% and below [73–75]. Beadless nanofibers were produced from PCL solutions with above 12% concentration in DMF/THF (1/1) solvent system [76–78]. Since the nanofiber diameter is mainly influenced by solution viscosity [79], the mean diameter of the beadless PCL nanofibers was 129.221 ± 39.24 nm, while the mean diameter of the beaded PCL nanofibers was 97.22 ± 21.18 nm. The beads were generally spherical, as can be clearly seen in Fig. 2b.

The SEM image representing the macroporous morphology of PHEMA cryogel is shown in Fig. 2c. Cryogels are three-dimensional hydrophilic networks that resemble their hydrogel counterparts. However, they differ from hydrogels with their large interconnected pores. Ice crystals formed during the polymerization created the supermacroporous PHEMA structure. The generally circular-shaped pores in the PHEMA cryogel structure can be attributed to the melting of the ice crystals due to the high surface tension of the solvent around the pore wall [80]. Macroscopically, soft spongy-like cryogels can be compressed, recovering to their original size and shape when the applied force is removed. This characteristic makes the cryogels eligible for the applications requiring insertable and removable biomaterials.

The microscopic architecture of PHEMA cryogel/beaded PCL nanofiber hybrid material is shown in Fig. 2d. The beaded PCL nanofibers contributed to microscale roughness for constructing the hierarchical hybrid structure. Nanofibers were observed inside the cryogel pores in the contact zone, where a hierarchical pore structure is formed. While the melting of ice crystals was responsible for the formation of the major pores, the random arrangement of the nanofibers at the junction layer caused the construction of the minor pores. As a result of morphological characterization, it is clear that the lotus-leaf-inspired strategy was successful in preparing two-layered hybrid material, including the PHEMA cryogel and beaded PCL nanofibers.

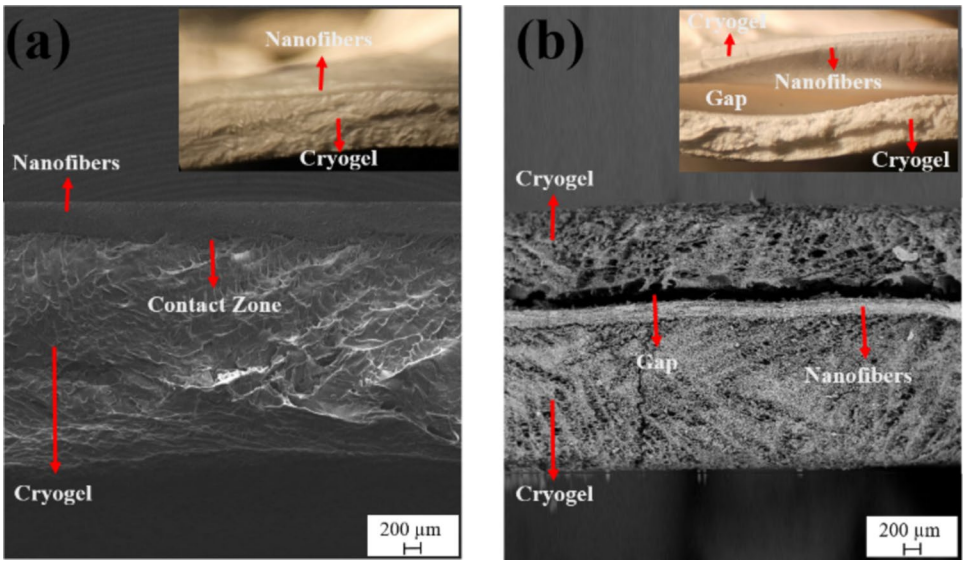

Fig. 3 Optical (10×) and SEM images (50×) of **a** the PHEMA cryogel/beaded PCL nanofiber hybrid material and **b** the PHEMA cryogel/beadless PCL nanofiber hybrid material

The thickness of PHEMA cryogel/beaded PCL nanofiber hybrid material was 3.19 ± 0.07 mm. However, it is possible to construct hybrid materials at different thicknesses using the same strategy and procedure.

Figure 3 shows the optical microscope and SEM images of the PHEMA cryogel/beaded PCL and PHEMA cryogel/beadless PCL nanofiber hybrid materials prepared at a low magnification ratio. Due to the surface roughness-induced hydrophobicity of the beaded PCL nanofibers, the wettability of the nanofibrous mat by the cryogelation solution decreased (Fig. 3a), as clearly shown in the SEM image. On the other hand, the PHEMA cryogelation solution was soaked up by the beadless PCL nanofibers due to the lack of surface roughness-induced hydrophobicity (Fig. 3b). The PHEMA cryogelation solution was absorbed by the beadless PCL nanofibers and the PHEMA cryogel and PCL nanofiber layers were separated forming a gap after drying at room temperature. However, PHEMA cryogel/beaded PCL nanofiber hybrid material was stable even after drying owing to the strong adhesion of PHEMA cryogel to the beaded PCL nanofibers. Consequently, it was clear that the applied strategy was successful in preparing layered cryogel/beaded nanofiber hybrid structures.

The FTIR spectrum of the PHEMA cryogel layer of the PHEMA cryogel/beaded PCL nanofiber hybrid material is given in Fig. 4. In the spectrum, the absorption band resulting from the stretching of O–H groups belonging to HEMA was observed at 3309 cm^{-1}. The absorption bands observed at 2943 cm^{-1}, 1718 cm^{-1}, and 1153 cm^{-1} belong to the C–H alkyl, carbonyl groups (C = O), and C–O bonds stretching, respectively [81].

The surface roughness-induced hydrophobicity created by beaded PCL nanofibers was also demonstrated via WCA measurements—the high contact angle results from

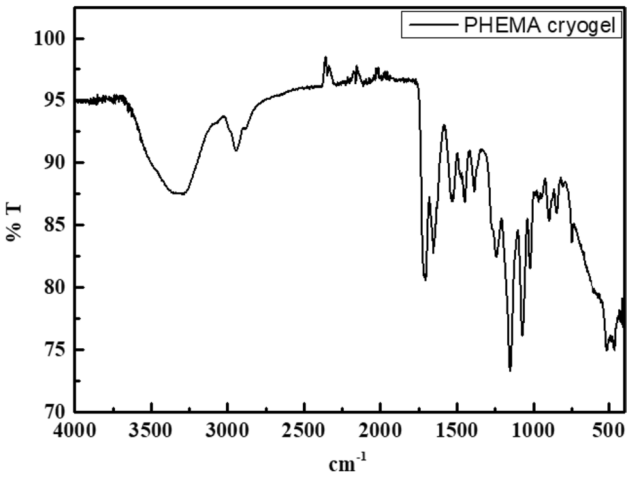

Fig. 4 The FTIR spectrum of PHEMA cryogel

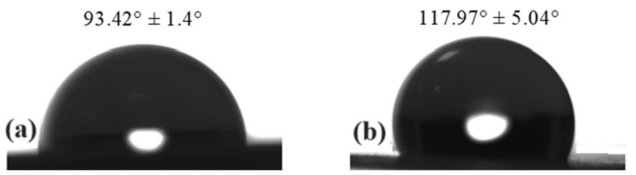

Fig. 5 WCAs of **a** the beadless PCL nanofibers and **b** the beaded PCL nanofibers

roughness and surface chemistry [50]. Figure 5 shows the WCAs of the beaded and beadless PCL nanofibers. The WCA of beadless (Fig. 5a) and beaded (Fig. 5b) PCL nanofibers was 93.42° ± 1.4° and 117.97° ± 5.04°, respectively, demonstrating that micro-sized beads in the PCL nanofibers increased the WCA. The hydrophobicity of the

beaded PCL surface resulted in a contact zone between PHEMA cryogel and the beaded PCL nanofiber without the absorption of PHEMA cryogelation solution by PCL nanofibers.

3.1.2 Porosity and Swelling Kinetics

In tissue regeneration and new tissue formation, the material's porosity plays an important role, enabling cell attachment and ingrowth and supporting the matrix's neovascularization [82]. At the same time, it is essential for drug release studies in terms of providing high drug absorption capacity and drug diffusion. The prepared PHEMA cryogel/beaded PCL nanofiber hybrid material has a cryogel layer with a usage potential for cell attachment and proliferation, depending on the targeted application. Therefore, the total porosity and the pore size distribution of the PHEMA cryogel were determined via mercury porosimetry. The ideal pore size ranges from 5 to 350 µm depending on the cell type/target in tissue regeneration [83]. The total porosity was 64.42%, which is in the preferred range of 60 to 90% for cell adhesion, migration, and proliferation, and the pore size was in the range of 5–200 µm, matching the human cell sizes [84]. The pore size distribution graph of the PHEMA cryogel is given in Fig. 6.

The swelling behavior of a biomaterial is also determinative in biomedical applications such as tissue engineering scaffolds, drug release, and wound dressing. Swelling is especially crucial for blood and wound extrudates absorption, the transference of nutrients and metabolites, and drug diffusion and release. Biomaterials with high swelling capacity have been widely used in full-thickness skin wound healing, tissue regeneration, and drug delivery. On the other hand, non-swelling biomaterials play critical roles in tissue adhesives, internal soft-tissue wound healing, and bioelectronics, owing to their durable macroscopic size and physical performance in a physiological environment [85]. Therefore, the swelling kinetics of the PHEMA cryogel/beaded PCL nanofiber hybrid material were investigated and compared to those of bare beaded PCL nanofibers and PHEMA cryogel. The obtained results are depicted in Fig. 7. The beaded PCL nanofibers' swelling ratio increased and reached its maximum (267.77%) within the first 30 min. PCL is hydrophobic, and its porosity is lower than macroporous PHEMA cryogel, consisting of pores in the range of 5–200 µm in diameter. Therefore, the beaded PCL nanofibrous mat swelled lower than the PHEMA cryogel and the hybrid material. PHEMA is highly hydrophilic and porous; thus, its swelling ratio was very high (381.83%) compared to beaded PCL nanofibers. The maximum swelling ratio of the PHEMA cryogel/beaded PCL nanofiber hybrid material was 509.69% and reached after 180 min. The swelling ratio of the hybrid biomaterial is slightly smaller than the total swelling ratio of PHEMA cryogel and beaded PCL nanofibers, probably because the strong attachment of the layers prevented their swelling as

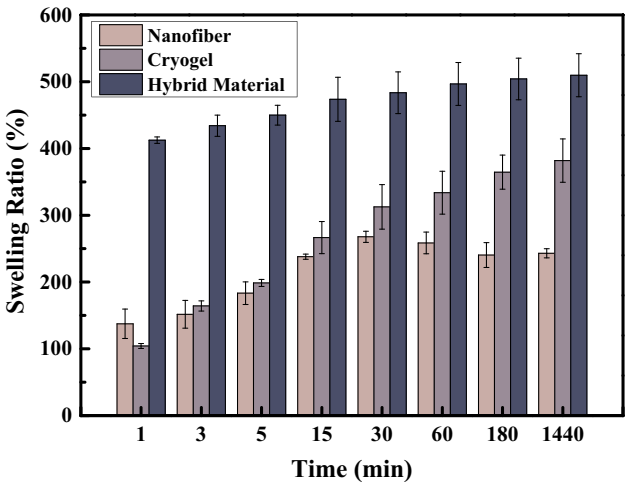

Fig. 7 Swelling kinetics of the beaded PCL nanofiber, PHEMA cryogel and PHEMA cryogel/beaded PCL nanofiber hybrid material

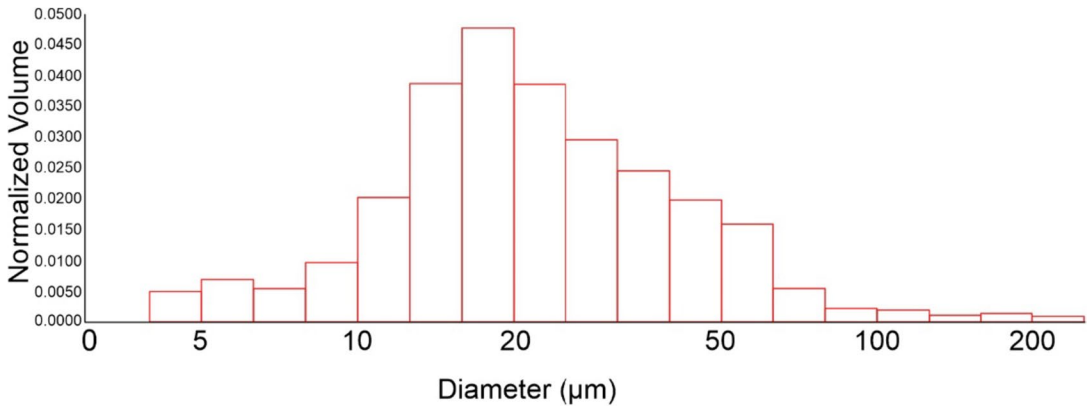

Fig. 6 Pore size distribution of the PHEMA cryogel

it occurred when they were free. As a result, the swelling ratio of prepared was eligible for biomedical applications.

4 Conclusion

In this study, a new strategy based on the lotus effect was developed to construct a cryogel/nanofiber hybrid material. The lotus effect was acquired by bead-on-string nanofibers produced with the appropriate solution and process parameters during electrospinning. Cryogel and nanofibers layers were PHEMA and beaded PCL, respectively. Since the PCL nanofibers were beaded, the PHEMA cryogelation solution was exposed to the lotus effect created by micro-sized beads of the nanofibers. A good adhesion was achieved between the PHEMA cryogel and the beaded PCL nanofibers. The roughness resulting from the beaded PCL nanofibers also caused an increase in the surface area contacting with the PHEMA cryogel. The total porosity (64.42%), pore size distribution (5–200 μm), and swelling ratio (509.69%) of the PHEMA cryogel were eligible for biomaterial applications. When the beadless PCL nanofibers was used as a layer in the hybrid material, the PHEMA cryogelation solution was absorbed by the nanofibers, and the layers were separated after drying. As a result, a new lotus-leaf-inspired strategy was developed to prepare cryogel/nanofiber hybrid materials, which can simultaneously enable drug loading and new tissue generation. The developed hybrid material's porosity, swelling capacity, and morphological properties show a lot of promise for wound closure, including drug release and bleeding control, taking advantage of the hemostatic properties of nanofibers and the absorption capacity of cryogel. In future studies, the cryogel/nanofiber hybrid materials, which will be prepared via the developed strategy, will be used in different applications such as drug release, wound dressing, and bone tissue engineering to demonstrate their usability in the biomedical area.

Acknowledgements This study was supported financially by Bursa Uludag University Scientific Research Projects (BAP) Unit (FHIZ-2021-627). We offer our gratitude for their support.

Author Contributions DK: investigation, experimentation. BO: methodology, validation, writing. EK: methodology, writing, supervision.

Funding Open access funding provided by the Scientific and Technological Research Council of Türkiye (TÜBİTAK). This work was supported by Bursa Uludag University (Project Number: FHIZ-2021-627).

Data Availability The data supporting the findings of this study are available within the article and/or from the authors upon reasonable request.

Declarations

Conflict of Interest The authors declare that there is no conflict of interests regarding the publication of this article.

Ethical Approval Not applicable.

Consent for Publication All the authors consented to this publication.

Consent to Participate Not applicable.

Open Access This article is licensed under a Creative Commons Attribution 4.0 International License, which permits use, sharing, adaptation, distribution and reproduction in any medium or format, as long as you give appropriate credit to the original author(s) and the source, provide a link to the Creative Commons licence, and indicate if changes were made. The images or other third party material in this article are included in the article's Creative Commons licence, unless indicated otherwise in a credit line to the material. If material is not included in the article's Creative Commons licence and your intended use is not permitted by statutory regulation or exceeds the permitted use, you will need to obtain permission directly from the copyright holder. To view a copy of this licence, visit http://creativecommons.org/licenses/by/4.0/.

References

1. H. Cheng, Y. Li, B. Wang, Z. Mao, H. Xu, L. Zhang, Y. Zhong, X. Sui, Cellulose (2018). https://doi.org/10.1039/c001939a
2. E.T. Jiann Chong, J.W. Ng, P.C. Lee, BIO Integr. (2023). https://doi.org/10.15212/bioi-2022-0009
3. R. Rasouli, A. Barhoum, M. Bechelany, A. Dufresne, Macromol. Biosci. (2019). https://doi.org/10.1002/mabi.201800256
4. T.M. Henderson, K. Ladewig, D.N. Haylock, K.M. McLean, A.J. O'Connor, J. Mater. Chem. B. (2013). https://doi.org/10.1039/C3TB20280A
5. Z.M. Huang, Y.Z. Zhang, M. Kotaki, S. Ramakrishna, Compos. Sci. Technol. (2003). https://doi.org/10.1016/S0266-3538(03)00178-7
6. G. Coşkun, E. Karaca, M. Ozyurtlu, S. Özbek, A. Yermezler, İ Çavuşoğlu, Bio-Med. Mater. Eng. (2014). https://doi.org/10.3233/BME-130956
7. M. Gorji, A.A.A. Jeddi, A.A. Gharehaghaji, J. Appl. Polym. Sci. (2012). https://doi.org/10.1002/app.36611
8. B. Yang, M. Hao, Z. Huang, Z. Chen, Y. Liu, Fiber Polym. (2023). https://doi.org/10.1007/s12221-023-00110-1
9. K. Gao, X. Hu, C. Dai, T. Yi, Mat. Sci. Eng. B (2006). https://doi.org/10.1016/j.mseb.2006.03.035
10. M.İ Altuntuğ Cesur, B. Osman, E. Tümay Özer, D. Kanmaz, M. Baykara, E. Karaca, Int. J. Polym. Mater. Polym. (2023). https://doi.org/10.1080/00914037.2023.2213387
11. A. Ahmed, M. Zhang, S. Li, L. Xu, Fiber Polym. (2023). https://doi.org/10.1007/s12221-023-00283-9
12. J. Yekrang, L. Mohseni, H. Etemadi, Fiber Polym. (2023). https://doi.org/10.1007/s12221-023-00100-3
13. A. Greiner, J.H. Wendorff, Angew. Chem. Int. Edit. (2007). https://doi.org/10.1002/anie.200604646
14. D. Li, X. Younan, Adv. Mater. (2004). https://doi.org/10.1002/adma.200400719
15. D. Kanmaz, H.A.K. Toprakci, H. Olmez, O. Toprakci, Mater. Sci. Res. India (2018). https://doi.org/10.13005/msri/150304
16. M. Rajithasri, P. Rajkumar, Pharma Innov. J. **11**, 6 (2022)

17. A.M. Grumezescu, in *Organic Materials as Smart Nanocarriers for Drug Delivery*. ed. by G.C. Patel, B.K. Yadav (William Andrew, USA, 2018), p.147
18. T.X. Li, L. Wang, Y.F. Huang, B.J. Xin, S. Liu, J. Biomater. Sci.-Polym. E. (2020). https://doi.org/10.1080/09205063.2020.1753932
19. X. Tian, H. Bai, Y. Zheng, L. Jiang, Adv. Funct. Mater. (2011). https://doi.org/10.1002/adfm.201002061
20. R. Huang, Z. He, Y. Bian, Z. Lei, H. Wang, Y. Long, M. Hu, J. Li, L. Xu, J. Li, X. Li, J. Biomed. Nanotechnol. (2019). https://doi.org/10.1166/jbn.2019.2865
21. P. Pal, P. Dadhich, P.K. Srivas, B. Das, D. Maulik, S. Dhara, Biomater. Sci.-UK (2017). https://doi.org/10.1039/C7BM00174F
22. J. Pu, F. Yuan, S. Li, K. Komvopoulos, Acta Biomater. (2015). https://doi.org/10.1016/j.actbio.2014.11.014
23. H.Y. Lin, S.H. Chen, S.H. Chang, S.T. Huang, J. Biomater. Sci.-Polym. E. (2015). https://doi.org/10.1080/09205063.2015.1061350
24. R. Wu, R.A. Niamat, B. Sansbury, M. Borjigin, Fibers (2015). https://doi.org/10.3390/fib3030296
25. S. Haldar, A. Sharma, S. Gupta, S. Chauhan, P. Roy, D. Lahiri, Mater. Sci. Eng. C (2019). https://doi.org/10.1016/j.msec.2019.110140
26. R.A. Franco, Y.K. Min, H.M. Yang, B.T. Lee, J. Biomater. Appl. (2013). https://doi.org/10.1177/0885328211416527
27. A. Zonari, M.T. Cerqueira, S. Novikoff, A.M. Goes, A.P. Marques, V.M. Correlo, R.L. Reis, Macromol. Biosci. (2014). https://doi.org/10.1002/mabi.201400005
28. M.N. Nicholas, M.G. Jeschke, S. Amini-Nik, Tissue Eng. Pt A. (2016). https://doi.org/10.1089/ten.tea.2015.0536
29. R. Guo, J. Teng, S. Xu, L. Ma, A. Huang, C. Gao, Wound Repair Regen. (2014). https://doi.org/10.1111/wrr.12171
30. F.H. Lin, J.C. Tsai, T.M. Chen, K.S. Chen, J.M. Yang, P.L. Kang, T.H. Wu, Mater. Chem. Phys. (2007). https://doi.org/10.1016/j.matchemphys.2006.11.017
31. E.V. Solovieva, A.Y. Teterina, O.I. Klein, V.S. Komlev, A.A. Alekseev, A.A. Panteleyev, Biomed. Mater. (2020). https://doi.org/10.1088/1748-605X/abb524
32. G. Ertürk, B. Mattiasson, J. Chromatogr. A (2014). https://doi.org/10.1016/j.chroma.2014.05.055
33. A. Kumar, V. Bansal, J. Andersson, P.K. Roychoudhury, B. Mattiasson, J. Chromatogr. A (2006). https://doi.org/10.1016/j.chroma.2005.08.094
34. V.I. Lozinsky, F.M. Plieva, I.Y. Galaev, B. Mattiasson, Bioseparation (2001). https://doi.org/10.1023/A:1016386902611
35. Y.A. Petrenko, R.V. Ivanov, V.I. Lozinsky, A.Y. Petrenko, Bullet. Exp. Biol. Med.+ (2011). https://doi.org/10.1007/s10517-011-1185-3
36. B.M. Carvalho, L.M. Carvalho, W.F. Silva Jr., L.A. Minim, A.M. Soares, G.G. Carvalho, S.L. da Silva, Food Chem. (2014). https://doi.org/10.1016/j.foodchem.2014.01.010
37. H. Alkan, Hacettepe J.Biol. Chem. (2015). https://doi.org/10.15671/HJBC.20154314240
38. Y.N. Martinez, L. Piñuel, G.R. Castro, J.D. Breccia, Appl. Biochem. Biotechnol. (2012). https://doi.org/10.1007/s12010-012-9554-6
39. M.B. Dainiak, A. Kumar, I.Y. Galaev, B. Mattiasson, Proc. Natl. Acad. Sci. U.S.A. (2006). https://doi.org/10.1073/pnas.050843210
40. N. Şahiner, S. Demirci, M. Şahiner, S. Ashle, H. Al-Lohedan, J. Environ. Manage. (2015). https://doi.org/10.1016/j.jenvman.2015.01.023
41. S. Sa'adon, M.N.M. Ansari, S.I.A. Razak, A.H.M. Yusof, A.A.M. Faudzi, S. Sagadevan, N.H.M.N. Nayan, J.S. Anand, K.A.M. Amin, Pharmaceutics (2021). https://doi.org/10.3390/pharmaceutics13111900
42. S.M. Andrabi, P. Singh, S. Majumder, A. Kumar, Chem. Eng. J. (2021). https://doi.org/10.1016/j.cej.2021.130219
43. S. Mousavi, F. Deuber, S. Petrozzi, L. Federer, M. Aliabadi, F. Shahraki, C. Adlhart, Colloid Surface A. (2018). https://doi.org/10.1016/j.colsurfa.2018.03.052
44. F. Deuber, S. Mousavi, M. Hofer, C. Adlhart, ChemistrySelect (2016). https://doi.org/10.1002/slct.201601084
45. S. Mousavi, L. Filipova, J. Ebert, F.J. Heiligtag, R. Daumke, W. Loser, B. Ledergerber, B. Frank, C. Adlhart, Sep. Purif. Technol. (2022). https://doi.org/10.1016/j.seppur.2021.120273
46. Y. Ziai, F. Petronella, C. Rinoldi, P. Nakielski, A. Zakrzewska, T.A. Kowalewski, W. Augustyniak, X. Li, A. Calogero, I. Sabała, B. Ding, L. De Sio, F. Pierini, NPG Asia Mater. (2022). https://doi.org/10.1038/s41427-022-00365-9
47. P. Nakielski, S. Pawłowska, C. Rinoldi, Y. Ziai, L. De Sio, O. Urbanek, K. Zembrzycki, M. Pruchniewski, M. Lanzi, E. Salatelli, A. Calogero, T.A. Kowalewski, A.L. Yarin, F. Pierini, ACS Appl. Mater. Int. (2020). https://doi.org/10.1021/acsami.0c13266
48. Y. Ziai, M. Lanzi, C. Rinoldi, S.S. Zargarian, A.B. Zakrzewska, A. Kosik-Koziol, P. Nakielski, F. Pierini, Nanoscale Adv. (2024). https://doi.org/10.1039/D3NA01022H
49. S. Sa'adon, S.I. Abd Razak, K. Fakhruddin, Procedia Comput. Sci. (2019). https://doi.org/10.1016/j.procs.2019.09.027
50. N. Nuraje, W.S. Khan, Y. Lei, M. Ceylan, R. Asmatulu, J. Mater. Chem. A. (2013). https://doi.org/10.1039/C2TA00189F
51. G. Zhang, P. Wang, X. Zhang, C. Xiang, L. Li, J. Polym. Sci. Polym. Phys. (2019). https://doi.org/10.1002/polb.24795
52. H. Fong, I. Chun, D.H. Reneker, Polymer (1999). https://doi.org/10.1016/S0032-3861(99)00068-3
53. K.H. Lee, H.Y. Kim, M.S. Khil, Y.M. Ra, D.R. Lee, Polymer (2003). https://doi.org/10.1016/S0032-3861(02)00820-0
54. T. Lin, Novel Aspects of Nanofibers, ed. By H. Zhao, H. Chi, (IntechOpen, United Kingdom, 2018)
55. G. Yang, X. Li, Y. He, J. Ma, G. Ni, S. Zhou, Prog. Polym. Sci. (2018). https://doi.org/10.1016/j.progpolymsci.2017.12.003
56. J.J. Huang, Y. Tian, R. Wang, M. Tian, Y. Liao, Sep. Purif. Technol. (2020). https://doi.org/10.1016/j.seppur.2019.116377
57. J. Santillan, E.A. Dwomoh, Y.G. Rodríguez-Avilés, S.A. Bello, E. Nicolau, ACS Appl. Bio Mater. (2019). https://doi.org/10.1021/acsabm.8b00628
58. S. Somvipart, S. Kanokpanont, R. Rangkupan, J. Ratanavaraporn, S. Damrongsakkul, Int. J. Biol. Macromol. (2013). https://doi.org/10.1016/j.ijbiomac.2013.01.006
59. Y.D. Ding, D. Xu, H. Shao, T. Cong, X. Hong, H.Y. Zhao, Fiber Polym. (2019). https://doi.org/10.1007/s12221-019-9040-7
60. Y. Li, Y. Wang, E.Y.B. Pun, H. Lin, Opt. Mater. Express (2018). https://doi.org/10.1364/OME.8.000276
61. X. Li, Z. Zhuang, D. Qi, C. Zhao, Sensor Actuat B-Chem. (2021). https://doi.org/10.1016/j.snb.2020.129239
62. G.M. Tan, X.Y. Xue, Z.G. Zhu, J.S. Li, ACS Est Water. (2021). https://doi.org/10.1021/acsestwater.1c00087
63. G. Uzunoğlu, Düşük Molekül Ağırlıklı Heparin Takılı Phema Kriyojel İle Kandan Kolesterol Uzaklaştırılması, Master's Thesis, Hacettepe University, Ankara, Türkiye (2013)
64. B. Azimi, P. Nourpanah, M. Rabiee, S. Arbab, J Eng Fiber Fabr. (2014). https://doi.org/10.1177/155892501400900309
65. S.M. Espinoza, H.I. Patil, E.S.M. Martinez, R.C. Pimentel, P.P. Ige, Int. J. Polym. Mater. Po. (2019). https://doi.org/10.1080/00914037.2018.1539990
66. N. Obregon, V. Agubra, M. Pokhrel, H. Campos, D. Flores, D. De la Garza, Y. Mao, J. Macossay, M. Alcoutlabi, Fibers (2016). https://doi.org/10.3390/fib4020020
67. L. Alberto, L. Kalluri, J. Qu, Y. Zhao, Y. Duan, Materials (2023). https://doi.org/10.3390/ma16052122
68. R.N. Wenzel, Ind. Eng. Chem. **28**(8), 988–994 (1936)

69. A.B.D. Cassie, S. Baxter, Trans. Faraday Soc. **40**, 546–551 (1944)
70. G. McHale, Langmuir (2003). https://doi.org/10.1021/la701167
71. K.S. Athira, P. Sanpui, K. Chatterjee, J.Polym. Biopolym. Phys. Chem. (2014). https://doi.org/10.12691/jpbpc-2-4-1
72. J.M. Deitzel, J. Kleinmeyer, D.E.A. Harris, N.B. Tan, Polymer (2001). https://doi.org/10.1016/S0032-3861(00)00250-0
73. N. Bölgen, Y.Z. Menceloğlu, K. Acatay, I. Vargel, E. Pişkin, J Biomat Sci-Polym E. (2005). https://doi.org/10.1163/156856205774576655
74. C.M. Hsu, S. Shivkumar, J. Mater. Sci. (2004). https://doi.org/10.1023/B:JMSC.0000025826.36080.cf
75. Y. Liu, S. Li, W. Lan, M.A. Hossen, W. Qin, K. Lee, Mater. Today Adv. (2021). https://doi.org/10.1016/j.mtadv.2021.100173
76. W.J. Li, R.L. Mauck, J.A. Cooper, X. Yuan, R.S. Tuan, J. Biomech. (2007). https://doi.org/10.1016/j.jbiomech.2006.09.004
77. W.J. Li, H. Chiang, T.F. Kuo, H.S. Lee, C.C. Jiang, R.S. Tuan, J Tissue Eng Regen M. (2009). https://doi.org/10.1002/term.127
78. F. Croisier, A.S. Duwez, C. Jérôme, A.F. Léonard, K.O. Van Der Werf, P.J. Dijkstra, M.L. Bennink, Acta Biomater. (2012). https://doi.org/10.1016/j.actbio.2011.08.015
79. R. Stepanyan, A.V. Subbotin, L. Cuperus, P. Boonen, M. Dorschu, F. Oosterlinck, M.J.H. Bulters, Polymer (2016). https://doi.org/10.1016/j.polymer.2016.05.045
80. M. Bakhshpour, N. Idil, I. Perçin, A. Denizli, Appl. Sci. (2019). https://doi.org/10.3390/app9030553
81. K. Şarkaya, A. Allı, J. Porous Mater. (2021). https://doi.org/10.1007/s10934-021-01037-9
82. I.M. El-Sherbiny, M.H. Yacoub, Global Cardiol. Sci. Pract. (2013). https://doi.org/10.5339/gcsp.2013.38
83. S. Yang, K.F. Leong, Z. Du, C.K. Chua, Tissue Eng. (2001). https://doi.org/10.1089/107632701753337645
84. Y.Q. Liu, J.W. Feng, C.C. Zhang, Y. Teng, Z. Liu, J.H. He, J. Therm. Sci. (2018). https://doi.org/10.2298/TSCI1804637L
85. W. Feng, Z. Wang, Adv. Sci. (2023). https://doi.org/10.1002/advs.202303326